THE JOURNAL OF PHYSICAL CHEMISTRY C

Article

pubs.acs.org/JPCC

Spectroscopy and Ultrafast Vibrational Dynamics of Strongly Hydrogen Bonded OH Species at the α-$Al_2O_3(11\bar{2}0)/H_2O$ Interface

Aashish Tuladhar,[†] Shalaka Dewan,[†] James D. Kubicki,[‡] and Eric Borguet*[,†]

[†]Department of Chemistry, Temple University, 1901 N. 13th Street, Philadelphia, Pennsylvania 19122, United States

[‡]Department of Geosciences, The Earth and Environmental Systems Institute, The Pennsylvania State University, University Park, Pennsylvania 16802, United States

Supporting Information

ABSTRACT: Frequency and time-resolved vibrational sum frequency generation (vSFG) are used to investigate the behavior of water at the α-$Al_2O_3(11\bar{2}0)$ surface. In addition to the typical water OH peaks (~3200 and ~3400 cm^{-1}), the α-$Al_2O_3(11\bar{2}0)/H_2O$ interface shows an additional red-shifted feature at ~3000 cm^{-1}. Addition of ions (0.1 M NaCl) largely attenuates the water OH peaks but has little effect on the 3000 cm^{-1} peak. The 3000 cm^{-1} feature is assigned to the O−H stretch of surface aluminol groups and/or interfacial water molecules that are strongly hydrogen bonded to the alumina surface. Density functional theory calculations were performed to test this assignment, revealing the presence of both associated and dissociated H_2O configurations (chemisorbed surface OH group) with frequencies at 3155 and 3190 cm^{-1}, respectively, at a hydrated α-$Al_2O_3(11\bar{2}0)$ surface. IR pump−vSFG probe measurements reveal that the interfacial OH species show very fast (<200 fs; bulk waterlike) vibrational relaxation dynamics, which is insensitive to surface charge and ionic strength, thus suggesting that the interfacial OH species at the α-$Al_2O_3(11\bar{2}0)/H_2O$ interface are in a highly ordered and strongly hydrogen-bonded environments. The observed fast vibrational relaxation of the interfacial OH species could be due to strong coupling between the 3000 cm^{-1} species and the interfacial water OH groups (3175 and 3450 cm^{-1}) via strong hydrogen bonds, dipole−dipole interaction between several interfacial OH groups (Förster type energy transfer), and/or ultrafast photoinduced proton transfer.

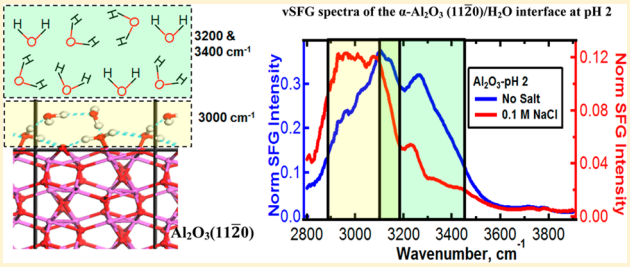

1. INTRODUCTION

Water is an interesting and important molecule, whose behavior is the object of much study. The key is to fully understand the nature of the extensive hydrogen bonding network of water, which dictates most of its unique properties.[1] The O−H stretch region has been shown to be an excellent probe of the hydrogen bonding network of bulk liquid water.[2−6] However, the understanding of interfacial water is less mature, mainly due to experimental challenges, most critical of which is the need to separate the huge bulk response from a small interfacial counterpart. Recent progress in nonlinear optics and the development of ultrashort mid-infrared sources[7] has allowed us to efficiently and selectively study the O−H stretch of interfacial water molecules.

The importance of understanding interfacial water is quite obvious, as it dictates many chemical, biological, and environmental processes.[8] One such area, where interfacial water plays a critical role, is the mineral/water interface, for example, the alumina/water interface which is the system under investigation in this study. Alpha alumina (α-Al_2O_3) is used in the ceramic industry (powder form) and as a substrate for thin-film formation. In heterogeneous catalysis, γ-alumina is used as a catalyst as well as a metallic catalyst support.[9,10] Corundum (a crystalline form of alumina) is a rock-forming mineral, and the adsorption of water on its surface is an important step in its geochemical transformation.

Under ambient conditions, the Al_2O_3 surface is protonated by atmospheric water and terminated with aluminol (Al−OH) groups. Upon contact with acidic and basic solutions, the Al−OH groups can undergo protonation and deprotonation reactions, creating surface groups (AlO^- and $AlOH_2^+$) that determine the interactions of solvent and solute with the alumina surface.[11] In addition to the surface Al−OH groups, the interfacial region also contains O−H groups from surrounding water molecules. The acid−base equilibrium at the alumina surface affects the identity and density of interfacial O−H groups. Therefore, a careful study of the O−H stretch region at the alumina/water interface is important to understand the interaction between alumina and the aqueous environment.[12]

Vibrational sum frequency generation (vSFG) is an interface specific nonlinear vibrational spectroscopy technique that has been widely used to inspect the mineral/water interface,[13−17] including the alumina (0001, $1\bar{1}02$, $11\bar{2}0$) surfaces.[18−20]

Special Issue: Kohei Uosaki Festschrift

Received: January 7, 2016

DOI: 10.1021/acs.jpcc.5b12486
J. Phys. Chem. C XXXX, XXX, XXX−XXX

Depending on the crystal orientation of the facet of alumina exposed to the aqueous layer, there is a difference in the surface termination and the coordination state of surface functional groups. For example, $Al_2O_3(0001)$ surface is terminated by Al_2O and displays a single functional group, Al_2OH, whereas, the $Al_2O_3(11\bar{2}0)$ surface is terminated by AlO, Al_2O, and Al_3O and therefore displays multiple functional groups, AlOH, Al_2OH, and Al_3OH.[21,22] Therefore, the behavior of adsorbed water molecules that directly interact with these various aluminol groups may be distinct. However, the vSFG studies at the (0001)[20] and $(11\bar{2}0)$[18] Al_2O_3 surfaces do not show significant variation in the OH stretch region, thus suggesting that the water adsorbed at these different types of surfaces is quite similar.

Interfacial water ordering was investigated next to the (001)[22] and (110)[21] surfaces of corundum by Catalano and the $(10\bar{1}0)$ and $(10\bar{1}1)$ surfaces of quartz[23] by Schlegel et al. using X-ray reflectivity measurements. [N.B. Corundum (110) is equivalent to alumina $(11\bar{2}0)$; it is common to not write the third Miller index due to its redundancy.[24]] These studies showed that the types of adsorbed water and hydrogen bonding environment are fundamentally different for each of these surfaces.[21−23] In a time-resolved IR spectroscopic study of the O−H stretch at the γ-alumina/ambient air interface, a vibrational mode was observed at 3080 cm^{-1} and assigned to a strongly hydrogen bonded chemisorbed species, which showed sub-picosecond (350 fs) population relaxation ascribed to photoinduced proton transfer reaction.[25] This result was in contrast with another study that assigned the 3685 cm^{-1} (~50 cm^{-1} fwhm) species to surface OH chemisorbed on another oxide, colloidal SiO_2, prepared in high content of physisorbed water, which showed a long vibrational energy relaxation time (~56 ps).[26] It follows that depending on the mineral and the face exposed, water interacts very differently with the surface. This difference in interaction should be observed while probing the O−H stretch. The vibrational frequency of strongly hydrogen bonded O−H stretch typically shows a red shift (stronger H-bond leads to a weaker O−H bond) and is expected to exhibit a fast vibrational relaxation (bulk ice shows faster vibrational relaxation than bulk water due to its stronger hydrogen bonding, which allows for faster energy transfer[27]).

The aim of the present study is to use frequency and time-resolved vSFG to investigate the interaction between water and the α-$Al_2O_3(11\bar{2}0)$ surface. Our vSFG spectra reveal that in addition to the water OH peaks (~3200 and ~3400 cm^{-1}) typically observed for the silica/water[15−17] and the alumina/water interface[18−20,28] there are two additional peaks: one is at ~3000 cm^{-1}, which we assign to strongly hydrogen bonded aluminol groups and/or interfacial water molecules that are strongly hydrogen bonded to the alumina surface, and the other peak is at ~3750 cm^{-1}, which is due to non-hydrogen bonded aluminol/water species. IR pump−vSFG probe measurements show that the strongly hydrogen-bonded OH species at the α-$Al_2O_3(11\bar{2}0)$/water interface undergo very fast (bulk waterlike) vibrational relaxation, and are insensitive to both surface charge (bulk water pH between 2 and 12) and ionic strength (NaCl concentration up to 0.5 M). Density functional theory (DFT) calculations reveal the presence of ~3100 cm^{-1} peaks originating from chemisorbed surface OH groups (aluminol groups) at a hydrated α-$Al_2O_3(11\bar{2}0)$ surface in associated and/or dissociated configuration, which is in agreement with our assignment of the 3000 cm^{-1} species observed in vSFG measurements.

2. EXPERIMENTAL SECTION

2.1. vSFG Experimental Setup. A one box Ti:sapphire oscillator + Regenerative amplifier (Coherent, LIBRA − F-1K-110-HE+) produces 5.0 mJ at 800 nm with a pulse duration of 120 fs at a repetition rate of 1 kHz. Ninety percent of the output (4.5 mJ) is used to pump a commercial OPA (Coherent, TOPAS-Prime HE) to produce 1.3 W of signal and idler. Tunable mid-infrared pulses are generated by collinear difference frequency mixing of signal and idler in $AgGaS_2$ (AGS) crystal with typical pulse energy of 20 μJ @ 3 μm (~200 cm^{-1} fwhm). The mid-IR energy was divided, using a silicon wedge, to produce pump and probe IR pulses with the ratio of 3:1. The remaining 5% of the regenerative amplifier output, spectrally narrowed to a fwhm of ~2.5 nm (38 cm^{-1}) using a narrow bandpass filter, is used as the visible light for vSFG measurements. A total internal reflection geometry (Figure S2) was employed in our vSFG experiments. The IR pump (8 μJ/pulse), IR probe (3 μJ/pulse), and visible (5 μJ/pulse) beams were incident at the surface with angles of 58°, 46°, and 51° and focused to beam waists of ~75, ~75, and ~200 μm, respectively. The vSFG signal was separated from the reflected visible light by short pass filters (Melles Griot) and was detected by a charge-coupled device detector (Princeton Instruments) coupled with a spectrograph (300i, Acton Research Corp.).

2.2. Steady-State vSFG Spectroscopy. In order to cover the entire spectral region of the O−H stretching region (3000−4000 cm^{-1}), the phase matching angle for DFG in AGS crystal was adjusted to generate broader mid-IR pulses (fwhm 450 cm^{-1}). The broad mid-IR pulses were spatially and temporally overlapped with the narrowband visible at the interface to produce vSFG spectra. The polarization combinations of PPP (denoting polarizations of the SF output, visible input, and infrared input, respectively) and SSP were used to record the steady-state vSFG spectra. The raw vSFG spectrum from the Al_2O_3/H_2O interface was normalized with respect to the IR pulse profile by dividing the raw sample spectrum by a reference spectrum acquired from the Al_2O_3−Au interface under otherwise identical conditions as discussed in Section 3 of the Supporting Information. The normalized spectrum was further corrected for wavelength dependence of Fresnel factor as discussed in Section 4 of the Supporting Information.

2.3. Time-Resolved vSFG (IR Pump−vSFG Probe). One-color IR pump−vSFG probe was employed to study the vibrational relaxation dynamics of the O−H stretch at the $Al_2O_3(11\bar{2}0)/H_2O$ interface. IR pulses (fwhm ~200 cm^{-1}) centered at 3100 cm^{-1} were generated by tuning the phase matching angle of the AGS crystal in order to investigate strongly hydrogen bonded species (3000−3300 cm^{-1}). The IR pump was P polarized. Initially, the intense P polarized IR pump pulse transfers population from the vibrational ground state ($\nu = 0$) to the first excited state ($\nu = 1$). The vSFG signal generated from the weaker probe IR and visible pulse monitors the ground-state population as a function of time. The position of zero time delay and instrument response function (fwhm 145 fs) was determined by the third-order cross-correlation ($\chi^{(3)}$) between IR pump, IR probe, and visible. The time delay between the IR probe and the visible was fixed, and the IR pump beam was scanned with respect to the IR probe and visible for acquiring the $\chi^{(3)}$ and time-resolved vSFG measurements. The data was recorded in 33 fs time steps using custom written programs with LABVIEW software. Each data point is

DOI: 10.1021/acs.jpcc.5b12486
J. Phys. Chem. C XXXX, XXX, XXX−XXX

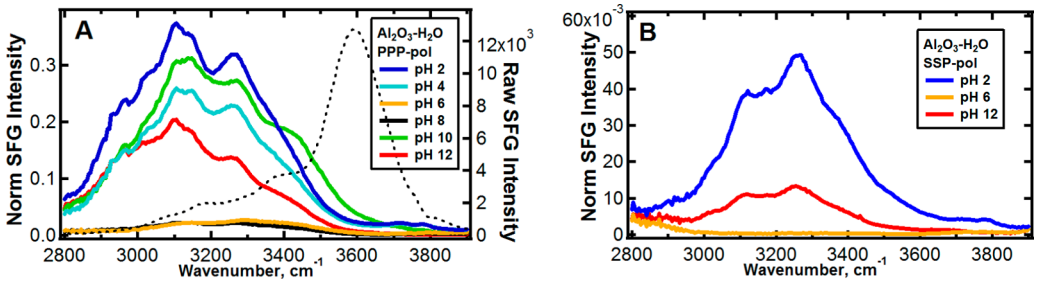

Figure 1. vSFG spectra of the α-$Al_2O_3(11\bar{2}0)/H_2O$ interface as a function of bulk pH (from 2−12) for (A) PPP polarization, and (B) SSP polarization. The black dotted line represents the IR pulse profile acquired from the Al_2O_3−Au interface. All the data have been normalized with respect to the IR pulse profile and corrected for the wavelength dependence of the Fresnel factors (Section 3 and 4 of the Supporting Information).

an average of 1000 laser pulses and the data shown in the figures represents an average of 3−5 scans. In order to account for the laser drift during typical scan time (15 min to 1 h), an external shutter was placed in the pump IR path so that at each acquisition time step, pumped (shutter open) and unpumped (shutter closed) dynamics data were recorded. The pumped data was divided by unpumped data to acquire normalized dynamics data.

2.4. Sample Preparation. α-Al_2O_3 hemicylindrical prisms with rectangular surface with $(11\bar{2}0)$ orientation (13 mm diameter and 27 mm length) were purchased from Meller Optics. Before each experiment, the prism was first cleaned with freshly prepared "piranha" solution (1 vol conc H_2O_2/3 vol. conc. H_2SO_4) for ∼30 min in a Teflon holder. (CAUTION: piranha is a very reactive mixture and must be handled with great care by using protective equipment (gloves, googles, and lab coat).) Then the prisms were rinsed with copious amounts of deionized water (>18.2 MΩ·cm resistivity, Thermoscientific Barnstead Easypure II purification system equipped with a UV lamp) and dried on a hot plate (while covered with aluminum foil). The prisms were then cleaned with a low-pressure RF air plasma for ∼15 min, after which they were kept in a pre-cleaned Teflon holder covered with aluminum foil until the experiment. The rectangular face of one of the prisms was coated with ∼100 nm Au film and used as a reference sample for normalization of raw data. The alumina prism was put in a flow-through sample holder, which has a small recess to allow solvent to come in contact with the rectangular face of the prism. The acidic solutions were prepared by diluting as received concentrated HCl (∼12.0 M, Fisher Scientific, analytical grade) in deionized H_2O. Basic solutions were prepared by diluting as-received 4.0 M NaOH solution (Fluke Analytical, analytical grade). The pH of the solutions was verified with a pH-meter (Oakton). The salt solutions were prepared by dissolving NaCl crystals (Fisher Scientific, >99.8%), which were heated to ∼500 °C overnight to remove impurities before use.

2.5. DFT Calculations. *Model Building.* From the experimental α-$Al_2O_3(11\bar{2}0)$ structure, cleavage of the bulk mineral to a 5 Al_2O_3-layer slab was achieved using the Surface Builder module of the Materials Studio software package (Accelrys Inc., San Diego, CA). The cleavage plane was adjusted through the model to break a minimum number of bonds. The monoclinic surface simulation cell was 14.60 Å × 9.82 Å × 39.27 Å with a slab thickness of 16.3545 Å and a vacuum thickness of 10 Å (Figure 1). The angle γ between the lattice vectors **a** and **b** was 95.8435°. Surface hydroxyl groups initially set in two configurations, an associated H_2O configuration with all terminal Al-(OH_2) groups and dissociated H_2O configuration with half of the H_2Os dissociated to form Al−OH and Al_2−OH surface hydroxyls. (Note that in both configurations, H_2Os originally bonded to an Al atom moved into physisorbed positions (Figure S1B, Supporting Information).) Energy minimizations of these models via relaxation of the ions with lattice parameters held fixed was performed in the Vienna Ab nnitio Simulation Package (VASP).[29,30] The composition was $Al_2O_{38}H_{16}$ in both cases so the energies could be compared directly.

Computational Methods. VASP was used to calculate all the structures and energies reported in this study.[29,30] Calculations were performed using the projector-augmented plane wave method[31,32] and the functional of Perdew−Burke−Ernzerhof (PBE).[33] The Al, O, and H atom pseudopotentials were supplied in the VASP library. An energy cutoff of 500 eV was applied throughout. With the simulation cell parameters fixed, a 2 × 2 × 1 *k*-point mesh for the static optimizations using the Monkhorst−Pack scheme was utilized. The self-consistent electron density was converged at each step to 1×10^{-4} eV and the energy minimization was terminated when the energy gradient was less than −0.02 eV/Å. Frequencies were calculated using the finite difference method in VASP with a step of 0.015 Å. Vibrational modes were visualized with the professional version of wxDragon (wxDragon is Copyright, 1994−2012 by Bernhard Eck).

3. RESULTS AND DISCUSSION

3.1. Steady-State vSFG Spectra of α-$Al_2O_3(11\bar{2}0)/H_2O$. *Effect of Surface Charge.* The normalized vSFG spectra (Figure 1) of the O−H stretch region for the α-$Al_2O_3(11\bar{2}0)$/H_2O system as a function of bulk pH (2−12) shows a trend consistent with that in the literature.[18] The minimum vSFG signal is observed at the point of zero charge (PZC) of alumina, which is reported to be pH 6−8.[18,20,28] Away from the PZC, the alumina surface charges creating an electric field that extends into the bulk water, which can orient the water via field-dipole interactions, resulting in increased vSFG signal. Three peaks at ∼3150, ∼ 3300, and ∼3740 cm^{-1} attributed to strongly hydrogen bonded, weakly hydrogen bonded, and free O−H species, respectively are observed in the SSP polarized vSFG spectra (Figure 1B), which is in agreement with the observation made by Shen et al.[18] The differences in the SSP polarized vSFG spectra observed in this study and the spectra of Shen et al. can be attributed to differences in the surface treatments, the experimental geometry (external reflection geometry employed by Shen et al. versus internal reflection geometry employed in this study), and the IR frequency region (Shen et al. do not probe below 3000 cm^{-1}). In addition, there is a small shoulder at ∼3000 cm^{-1}, which was also observed

DOI: 10.1021/acs.jpcc.5b12486
J. Phys. Chem. C XXXX, XXX, XXX−XXX

previously[18] but not assigned. The 3000 cm^{-1} peak is more prominent in the PPP polarized vSFG spectra (Figure 1A), which was not measured by the Shen group. This is in contrast to the normal water OH peaks (3150 and 3350 cm^{-1}), which is equally prominent in both SSP and PPP polarization combination. The difference in sensitivity of the SSP and PPP polarization combination toward the 3000 cm^{-1} species is discussed briefly in Section 5 of the Supporting Information. This behavior probably points toward difference in origin/symmetry property between the 3000 cm^{-1} species and normal water OH peaks (3150 and 3350 cm^{-1}). A detailed (polarization versus angle of incidence) study of the 3000 cm^{-1} species, similar to the one conducted by Wang et al.[34] at the air−water interface, is required to definitively resolve this question. The 3000 cm^{-1} feature becomes more obvious in the presence of ions (Figure 2), as discussed later.

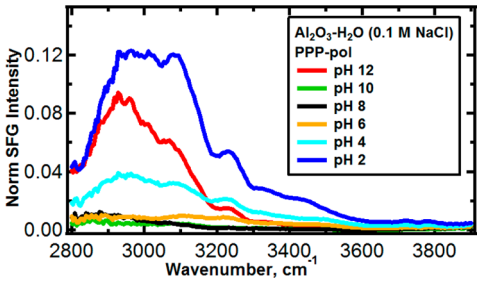

Figure 2. vSFG spectra of the α-$Al_2O_3(11\bar{2}0)/H_2O$ interface as a function of bulk pH (from 2−12) in the presence of 0.1 M NaCl. All the data have been normalized with respect to the IR pulse profile and corrected for the wavelength dependence of the Fresnel factor (Section 3 and 4 of the Supporting Information).

A similar red-shifted peak has been observed at the quartz/water,[35] and more frequently at the alumina/water interfaces.[11,36−39] For the quartz/water system,[35] the 3000 cm^{-1} peak was ascribed to "icelike structure of water" that is strongly hydrogen bonded with surface O−H groups. There have been numerous sighting of similar red-shifted peaks for the alumina/water system, most noticeable for the α-$Al_2O_3(11\bar{2}0)$[18,36] and γ-Al_2O_3.[25] In the latter oxide, the 3100 cm^{-1} peak was assigned to chemisorbed species (undissociated water molecules and aluminol groups), and its vibrational dynamics was measured at the alumina/air system that will be discussed later.[25] Interestingly, no 3000 cm^{-1} peak was reported in the vSFG study of α-$Al_2O_3(0001)/H_2O$ by Shen et al.[20] However, a molecular dynamics simulation study of α-$Al_2O_3(0001)/D_2O$[37] showed a prominent O−D stretch at 2200 cm^{-1} (corresponding to an O−H stretch at 3000 cm^{-1}), which was assigned to "icelike" water molecules donating strong hydrogen bonds to in-plane surface Al_2O−D group. In addition, the O−H stretch of bulk $AlO(OH)\cdot\alpha H_2O$ (boehmite, a precursor of alumina) shows a peak at 3098 cm^{-1}.[40]

Chemisorbed surface OH groups are not always observed in the vSFG spectra of mineral oxide/water interfaces. The absence of chemisorbed silanol (Si−OH) groups in most vSFG study of silica/water interface[15−17] could be due to the density of Si−OH groups compared to interfacial water molecules. At a silica surface, there are ∼4 O−H groups/nm^2, significantly less than the density of O−H groups from water (∼20 O−H groups/nm^2) at the interfacial layer.[41] Because the intensity of vSFG is proportional to the square of number density, the signal arising from the interfacial water OH groups is ∼25 times that from the surface silanol groups. This explains the absence of features corresponding to surface silanol groups in vSFG spectra of silica/water interfaces.[15−17] In contrast, the density of O−H groups due to surface aluminol species at the Al_2O_3 surface is much higher (∼13 O−H groups/nm^2)[42] and comparable to the density of OH groups due to interfacial water. Therefore, the detection of surface hydroxyl species is more likely at the α-$Al_2O_3(11\bar{2}0)/H_2O$ interface.

Effect of Ionic Strength. The effect of addition of ions on the vSFG spectra of the mineral/water interface has been investigated. The reduction in the overall vSFG signal is usually interpreted in terms of either screening of the surface charge or the disruption of the interfacial H-bonding network due to the presence of ions.[15,17] Similarly, the addition of 0.1 M NaCl (Figure 2) on the O−H stretch region of the α-$Al_2O_3(11\bar{2}0)/H_2O$ system reduces the overall vSFG signal at all bulk pHs. However, the extent of reduction in the vSFG signal is not uniform over the entire O−H stretch region, contrary to the silica/water system.[15] The vSFG intensity attenuates at ∼3150 and ∼3300 cm^{-1} such that the ∼3000 cm^{-1} species becomes the dominant peak (Figure 2). The free OH peak around ∼3750 cm^{-1} region remains even in the presence of ions. This observation suggests that the 3000 and ∼3750 cm^{-1} peaks arise from truly interfacial species and not from bulklike water sampled by the electric-field induced effects.[15,16]

The 3000 cm^{-1} peak can be due to two different kinds of interfacial OH groups:

(1) Chemisorbed surface OH groups that are formed when interfacial water molecules chemically bind to the surface to form aluminol groups and are strongly hydrogen bonded to the surrounding OH groups. The difference in attenuation of 3000 cm^{-1} peak compared to normal water OH peaks (∼3150 and 3350 cm^{-1}) upon addition of ions is consistent with this assignment. However, for the Al_2O_3/H_2O system, the surface aluminol groups have typically been observed around 3650−3750 cm^{-1} region (tiny peak near 3750 cm^{-1} in Figures 1 and 2).[12,18−20,43] At another oxide, hydrated colloidal SiO_2 sample, the chemisorbed surface OH group appeared at 3685 cm^{-1}.[26] The large difference in the OH stretch frequency (3000 versus 3750 cm^{-1}) for the two types of aluminol OH groups can be explained by the difference in their hydrogen bonding environment. The 3000 cm^{-1} aluminol group forms strong hydrogen bonds with the surrounding O−H groups, while the ∼3750 cm^{-1} aluminol groups are only weakly or non-hydrogen bonded, as previously reported.[12,18−20,43]

(2) OH of the interfacial water molecules that form strong hydrogen bonds with the surface aluminol groups. This assignment is supported by the observation that addition of ions slightly perturb the vSFG spectra even at 3000 cm^{-1} region (small intensity attenuation and some red shift in central frequency). If the surface aluminol groups were solely responsible for the 3000 cm^{-1} peak, the perturbation of 3000 cm^{-1} peak due to ions would be minimal. Also, similar water species with 3000 cm^{-1} frequency have been reported before at several mineral/water interfaces.[11,25,35,37,39]

An interesting observation is the effect of ions on the vSFG spectra at the α-Al_2O_3 $(11\bar{2}0)/H_2O$ interface as a function of bulk pH. It was recently shown that the attenuation of the vSFG spectra upon addition of ions at the silica/water interface is greatest at pH 7−8.[15] In this study, at the α-Al_2O_3 $(11\bar{2}0)/H_2O$ interface the effect of ions is largest (attenuation by a factor of 70) at pH 10 compared to attenuation by a factor of ∼3−4 at other pHs. In order to understand this effect, a

DOI: 10.1021/acs.jpcc.5b12486
J. Phys. Chem. C XXXX, XXX, XXX−XXX

detailed investigation of the acid/base chemistry of the different OH groups at the α-$Al_2O_3(11\bar{2}0)/H_2O$ interface is required, which is beyond the scope of this paper. We speculate that the variation in the effect of ions at different pH observed in this study is related to the protonation/deprotonation reaction of the surface aluminol groups.

Previously, it was reported that the adsorbed water next to the α-$Al_2O_3(11\bar{2}0)$ surface is more ordered than the adsorbed water next to the α-$Al_2O_3(0001)$ and quartz surfaces.[22] An important question is whether the presence of 3000 cm^{-1} species is unique to highly ordered and strongly hydrogen bonded water molecules next to the $(11\bar{2}0)$ mineral surface. Surprisingly, MD simulations of α-$Al_2O_3(0001)/D_2O$[37] showed a prominent O−D stretch at 2200 cm^{-1} (corresponding to an O−H stretch at 3000 cm^{-1}), which is in apparent contradiction with the vSFG study of α-$Al_2O_3(0001)/H_2O$ by Shen et al.,[20] where no intensity was observed in the 3000 cm^{-1} region. Similarly, vSFG studies show the 3000 cm^{-1} feature for the quartz/H_2O system[35] but not for the fused silica/H_2O system.[15,17] Clearly, steady-state vSFG alone is not sufficient to thoroughly understand the interaction between water and mineral surfaces, particularly in the strongly hydrogen bonded O−H stretch region (3000−3100 cm^{-1}). To obtain a more detailed understanding of the interaction between water and the α-$Al_2O_3(11\bar{2}0)$ surface and to investigate the origin of 3000 cm^{-1} species, we performed DFT calculations.

3.2. DFT Results. The DFT energy minimizations resulted in two stable structures (Figure S1A,B, Supporting Information) but the dissociated configuration was 4 kJ/mol lower in energy than the associated configuration. Energy minimizations do not account for entropic effects; therefore they do not provide a Gibbs free energy and relative activities of each type of surface configuration. Consequently, both associated and dissociated configurations are likely on the $(11\bar{2}0)$ surface. Vibrational frequency analysis with a 500 eV cutoff resulted in frequencies at 3155 to 3821 cm^{-1} and 2806 to 3852 cm^{-1} in the associated and dissociated configurations, respectively. The associated configuration frequency at 3155 cm^{-1} and a dissociated configuration frequency at 3190 cm^{-1} could both be responsible for the observed peak at 3000 cm^{-1}. These values are not scaled, and frequencies calculated in this manner tend to overestimate observed frequencies, largely due to anharmonic effects. For the associated configuration, the 3155 cm^{-1} vibration is due to an O−H stretch in an Al-(OH_2) group where one H is H-bonded to an Al_3O atom at a distance of 1.68 Å (Figure 3A). For the dissociated configuration, the 3190 cm^{-1} vibration is due to an O−H stretch in Al−OH group where one H is H-bonded to an O atom of an AlOH group at a distance of 1.63 Å (Figure 3B). Both of these modes could contribute to the observed peak at 3000 cm^{-1} because the peak is fairly broad. In addition, it is likely that both configurations are related because the H-bonding in the associated configuration could lead to the dissociated configuration by a simple H^+-transfer. Considering the strength of the H-bond in both configurations, H^+-hopping between sites is probable.

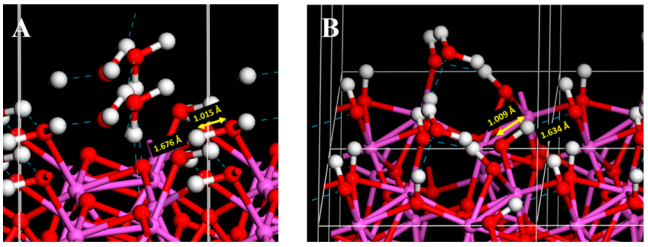

Figure 3. (A) Associated configuration vibrational mode at 3155 cm^{-1}, and (B) dissociated configuration vibrational mode at 3190 cm^{-1} at the hydrated α-$Al_2O_3(11\bar{2}0)$ surface.

3.3. Vibrational Relaxation Dynamics of the Strongly Hydrogen Bonded OH Stretch (3000−3300 cm^{-1}) at the α-$Al_2O_3(11\bar{2}0)/H_2O$ Interface. X-ray reflectivity studies predicted ordering and a strong hydrogen bonding environment for adsorbed water at the $Al_2O_3(11\bar{2}0)$ surface.[21] One way to investigate the extent of hydrogen bonding is by measuring the vibrational relaxation dynamics of the O−H stretch at the interface. The vibrational lifetime of an O−H stretch in a strongly hydrogen bonded and ordered environment would be shorter than for an O−H stretch in a weakly hydrogen bonded and disordered environment (ice shows faster vibrational relaxation dynamics than liquid water).[27]

To investigate the extent of ordering and hydrogen bonding environment of the interfacial OH species at the α-$Al_2O_3(11\bar{2}0)/H_2O$ interface, we measured the vibrational relaxation dynamics of the interfacial OH species using one color IR pump−vSFG probe, analogous to IR pump-IR probe spectroscopy (transient absorption technique), which has been used extensively to study vibrational dynamics of bulk water.[44−46] Both techniques measure the vibrational relaxation dynamics but differ in their sensitivity toward water in centrosymmetric and noncentrosymmetric environments. Therefore, IR pump−vSFG probe should measure the dynamics exclusively of the interfacial water molecules. We observe that the recovery of bleach in the vSFG signal is clearly double-exponential in nature (Figure 4) as seen previously by Bakker in their bulk water dynamics data,[46] and other IR pump−vSFG probe experiments on the O−H stretch of water.[8,47−49] Hence, a four-level system[8,49] (Figure S5, Supporting Information) can be used to describe the observed vSFG response for the O−H stretch dynamics; population

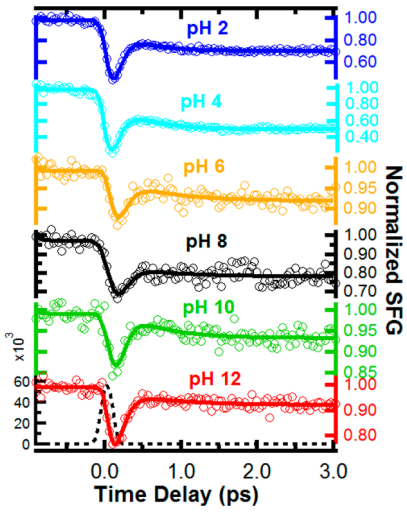

Figure 4. IR pump-vSFG probe vibrational dynamics of the interfacial OH species at the α-$Al_2O_3(11\bar{2}0)/H_2O$ interface for bulk pH 2, pH 4, pH 6, pH 8, pH 10, and pH 12. The solid line is the fit consistent with a four-level system (eq 1). The third-order cross-correlation between IR pump, IR probe, and visible is shown by the black dashed line and has a fwhm of ∼145 fs, suggesting IR pulse durations of ∼100 fs. P-polarized IR pump and PPP-polarized vSFG probe was used.

DOI: 10.1021/acs.jpcc.5b12486
J. Phys. Chem. C XXXX, XXX, XXX−XXX

Table 1. T_1 and T_{th} Lifetime Extracted from Fitting Time-Resolved vSFG Data for the α-$Al_2O_3(11\bar{2}0)/H_2O$ Interface for Bulk pH 2−12 Using Equation 1[a]

pH	2	4	6	8	10	12
T_1 (fs)	133 ± 19	155 ± 40	104 ± 17	110 ± 27	103 ± 16	127 ± 21
T_{th} (fs)	451 ± 91	433 ± 45	583 ± 164	586 ± 143	513 ± 68	579 ± 129

[a]The error bars are the standard deviation of the results of 3−6 independent experiments.

relaxes from the first excited state ($\nu = 1$) to an intermediate level, which then relaxes (thermalizes) toward a quasi-equilibrium state, where the excess energy is statistically distributed over all degrees of freedom. The IR pump−vSFG probe data can be fit to a numerical solution to the differential equation describing the four-level system[8,49] (Figure S5, Supporting Information), convolved with a Gaussian instrument response function, IRF(t), of the form:

$$I_{SFG} = \mathrm{IRF}(t)*[N_0(t) - N_1(t) + C_2N_2(t) + C_3N_3(t)]^2 \quad (1)$$

where, N_0, N_1, N_2, and N_3 are the populations of the $\nu = 0$, $\nu = 1$, $\nu = \nu^*$, and $\nu = 0^*$ states, respectively, and C_2 and C_3 are factors related to the nonlinear optical susceptibilities of the intermediate and final levels.[49]

From studies on bulk water, we know that the O−H stretching vibration in pure H_2O is delocalized due to the strong resonant coupling of vibrational modes, resulting in rapid spectral diffusion and fast intermolecular energy transfer.[50−52] Similarly, interfacial water (pure H_2O) at the silica/water interface showed frequency independent vibrational dynamics as a result of fast spectral diffusion,[47,53] which occurs on the time scale of <100 fs,[50,51] followed by silica surface charge dependent vibrational relaxation.[47,49,53] For the α-$Al_2O_3(11\bar{2}0)/H_2O$ interface, we also expect spectral diffusion to occur in sub-100 fs time scale (outside the resolution of our experiment), followed by vibrational relaxation through intra- and intermolecular energy transfer between the OH modes of water. The presence of strongly hydrogen bonded 3000 cm^{-1} OH groups is also likely to provide an additional pathway for vibrational relaxation through strong coupling between the 3000 cm^{-1} OH groups and the physisorbed water OH groups (3175 and 3450 cm^{-1}) and/or dipole−dipole interactions via Förster-type resonant vibrational energy transfer between the 3000 cm^{-1} OH species and other interfacial OH groups.

Effect of Surface Charge on Vibrational Dynamics. The effect of surface charge (Figure 4) on the vibrational relaxation of the interfacial OH species at the α-$Al_2O_3(11\bar{2}0)/H_2O$ interface was investigated and the time constants extracted from the fits are summarized in Table 1. The percent bleach observed varied between independent experiments and is discussed in Section 7 of the Supporting Information. The T_1 lifetime is short (comparable to bulk water) and insensitive to surface charge, that is, T_1 is short at all bulk pH values. This is very different from the behavior of the OH stretch at the fused silica surface.[47]

At a neutral silica surface, the interfacial OH groups showed slow dynamics (~570 fs) whereas at a negatively charged silica surface the observed dynamics was fast (~250 fs) and comparable to bulk water.[47] This was explained in terms of the difference in the vSFG probing depths for neutral compared to charged surfaces. A charged surface creates an electric field that extends into the bulk water, orienting and/or polarizing the water over the Debye length. Thus, water in bulklike environments, even away from the interface, can contribute to and even dominate the vibrational dynamics (T_1 = ~250 fs). On the contrary, at neutral silica surfaces, there is no electric field. Hence, vSFG, in the dipole approximation, is only sensitive to "truly" interfacial OH groups so that a slowing down of the vibrational lifetime of the excited OH stretch (T_1 = ~ 570 fs) was observed.[47] The reason provided for slow vibrational dynamics was incomplete solvation of the few interfacial water molecules that reduced the efficiency of intermolecular vibrational energy transfer to the surrounding environment.[47]

One would expect similar results at the α-$Al_2O_3(11\bar{2}0)/H_2O$ interface. At pH 2 and 12, where the alumina surface is positively and negatively charged, respectively, the measured dynamics should be representative of "bulklike" water and show fast relaxation. As expected, at charged alumina (pH 2 and 12), the T_1 lifetimes (Table 1) were fast, 138 and 130 fs, respectively. On the other hand close to the PZC (pH 6−8), vSFG should mainly probe OH groups next to the surface in the absence of a surface charge induced electric field. Therefore, we expected the vibrational dynamics of interfacial OH species to be slow (as in the case of silica/water). However, our results show that the T_1 lifetime at pH 6 and 8 is still very fast, 115 and 132 fs, respectively. This suggests that the excited interfacial OH groups at the α-$Al_2O_3(11\bar{2}0)$ surface can efficiently relax back to the ground state by transferring energy to its surrounding OH groups and/or by population transfer.

Water at the neutral silica surface[47] (at pH 2) and membrane bound water[54] shows slower vibrational relaxation dynamics (T_1 = ~600 fs) than bulk water (T_1 = ~200 fs) due to incomplete solvation and a consequently reduced efficiency of transfer of vibrational energy to the surrounding environment. Also, surface OH groups chemisorbed at colloidal SiO_2 surfaces in vacuum showed very slow vibrational relaxation (204 ps), which became much faster (56 ps) when the SiO_2 sample was prepared with a high content of physisorbed water.[26]

The question arises as to why the interfacial OH species at the α-$Al_2O_3(11\bar{2}0)/H_2O$ interface show fast vibrational dynamics comparable to bulk water even at the PZC of alumina (pH 6−8)? This could be due to the following possible reasons:

(1) At the charged α-$Al_2O_3(11\bar{2}0)$ interface, that is, pH 2, 4, 10, and 12, the vibrational dynamics of the OH stretch is fast and can be interpreted as water in bulklike environments contributing or even dominating the vibrational relaxation dynamics via efficient intra- and intermolecular energy transfer. However, at the neutral α-$Al_2O_3(11\bar{2}0)$ surface the vibrational dynamics of the few layers of interfacial OH groups is still fast possibly due to the presence of the strongly hydrogen bonded 3000 cm^{-1} species. At the neutral α-$Al_2O_3(11\bar{2}0)$ surface, intermolecular energy transfer between different OH groups (3000 and 3175 cm^{-1} OH species) via dipole−dipole interaction (Förster type energy transfer) could be the dominant mechanism of vibrational relaxation, leading to fast OH vibrational relaxation. In order for Förster type energy transfer to occur, there has to be spectral overlap between the

DOI: 10.1021/acs.jpcc.5b12486
J. Phys. Chem. C XXXX, XXX, XXX−XXX

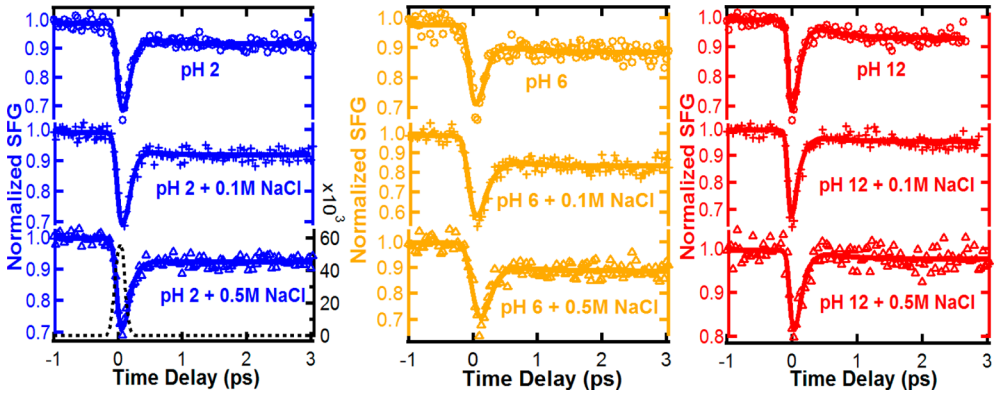

Figure 5. Effect of ions (0.1 M NaCl and 0.5 M NaCl) on the vibrational relaxation dynamics of the OH species at the α-$Al_2O_3(11\bar{2}0)/H_2O$ interface for bulk pH 2 (blue), pH 6 (yellow), and pH 12 (red). The solid line is the double exponential fit consistent with a four-level system (eq 1). The third-order cross-correlation between IR pump, IR probe, and visible is shown by the black dashed line and has a fwhm of ~145 fs, suggesting IR pulse durations of ~100 fs. P-polarized IR pump and PPP-polarized vSFG probe was used.

bands associated with different OH groups, which is possible for the 3000 and 3150 cm^{-1} species at the α-$Al_2O_3(11\bar{2}0)/H_2O$ interface. The similarity of time scale of vibrational relaxation at the charged and the neutral α-$Al_2O_3(11\bar{2}0)$ surface (Table 1) possibly points toward the Förster type energy transfer being the main mechanism of vibrational relaxation even at a charged alumina surface.

(2) The rate of vibrational relaxation not only depends on the density of hydrogen bonding partners but also on the strength of interaction between H-bond donors and acceptors. For example, the vibrational dynamics of bulk ice is faster than bulk water even though the number of hydrogen bonds is only marginally different.[27] The faster dynamics observed for bulk ice is due to its higher degree of ordering and stronger hydrogen bonding.[27] The presence of 3000 cm^{-1} OH group suggests that the hydrogen bonding environment at the α-$Al_2O_3(11\bar{2}0)/H_2O$ interface is strong, and possibly more ordered, as predicted by Catalano in his work.[21] Therefore, the strongly hydrogen-bonded OH groups at the α-$Al_2O_3(11\bar{2}0)$ surface show fast vibrational relaxation dynamics by efficiently transferring vibrational energy to acceptors (neighboring waters) via strong hydrogen -bonding interactions.

(3) A time-resolved study of water dynamics at γ-Al_2O_3/air interface observed a peak at 3080 cm^{-1} (close to the 3000 cm^{-1} feature of our study) that was assigned to chemisorbed species.[25] Transient absorption kinetics while pumping at 3000 cm^{-1} showed bleaching at 3080 cm^{-1} (decrease in population of $AlOH_2^+$) and induced absorption at ~3500 cm^{-1} (increase in population of AlOH) and 3000 cm^{-1} (increase in population of H_3O^+). The authors explained this in terms of photoinduced proton transfer from $AlOH_2^+$ to its neighboring water molecules according to the following

$$AlOH_2^+ + H_2O \rightleftharpoons AlOH + H_3O^+ \quad (2)$$

On the basis of this equilibrium, the fast relaxation of the interfacial OH species at the α-$Al_2O_3(11\bar{2}0)/H_2O$ interface observed in this study could indicate a photoinduced proton transfer mechanism[25] for the interfacial OH species, which would explain why the vibrational relaxation remains fast even at PZC for α-$Al_2O_3(11\bar{2}0)$ surface. However, this explanation is speculative at best and further experiments will be needed to confirm this as the dominant mechanism for vibrational relaxation.

Effect of Ionic Strength. Ions are known to be able to disrupt the hydrogen-bonding network and hence weaken the hydrogen bond strength and alter the OH vibrational relaxation dynamics.[55,56] It has been shown previously that the dynamics of water near ions are much slower than water in an ion-free environment.[56] Therefore, we investigated the effect of ions (0.1 and 0.5 M NaCl) on the vibrational dynamics of interfacial OH groups at the α-$Al_2O_3(11\bar{2}0)$ surface.

Ions at and near a charged interface attenuate (screen) the surface charge induced electric field that can align and/or polarize the water molecules. Alternatively, the presence of ions could also disrupt the hydrogen bond network as originally hypothesized by a silica dissolution rate study[57] and later supported by a vSFG study.[15] At the silica/water interface,[49] the addition of ions at pH 6 slowed down the dynamics of water, which was explained to be a consequence of the reduction in probing depth of vSFG due to increase in ionic strength. Above 10^{-2} M NaCl, the measured slow dynamics was representative of the few water layers next to the silica surface, which had fewer hydrogen bonding partners and hence showed slower dynamics.[49] In this study, the addition of ions has little to no effect on T_1 and T_{th} relaxation lifetime (Figures 5 and 6).

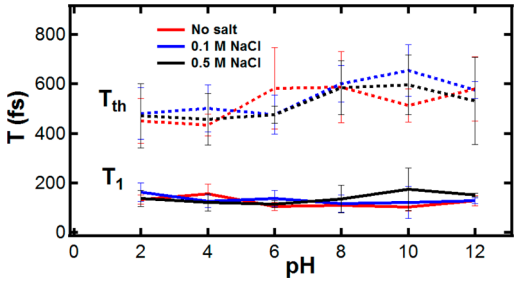

Figure 6. Effect of surface charge (pH 2−12) and ionic strength (0.1 M NaCl and 0.5 M NaCl) on T_1 and T_{th} vibrational lifetime of the interfacial OH species at the α-$Al_2O_3(11\bar{2}0)/H_2O$ interface.

At high ionic concentration (0.1 and 0.5 M NaCl), the vibrational dynamics of the first layers of interfacial OH groups is still fast (<200 fs). This result is consistent with the observation that the interfacial water at the α-$Al_2O_3(11\bar{2}0)$ surface is highly ordered and the vibrational relaxation of the OH groups is significantly influenced by the presence of strongly hydrogen bonded 3000 cm^{-1} OH species.

DOI: 10.1021/acs.jpcc.5b12486
J. Phys. Chem. C XXXX, XXX, XXX−XXX

4. CONCLUSION

In conclusion, we have investigated the interaction between water and the α-$Al_2O_3(11\bar{2}0)$ surface using vSFG spectroscopy and DFT calculations. Static vSFG spectra revealed the presence of strongly hydrogen-bonded species at 3000 cm^{-1}, which is red shifted compared to typical hydrogen-bonded interfacial water peaks (~3200 and 3400 cm^{-1}). The addition of ions does not significantly perturb the vSFG intensity of this feature, which indicates its interfacial origin and strong interaction with the surface. DFT calculations predict the presence of water molecules in associated and dissociated configurations at the hydrated α-$Al_2O_3(11\bar{2}0)$ surface with 3155 and 3190 cm^{-1} frequencies, respectively, which is close to the ~3000 cm^{-1} feature observed in our vSFG results. On the basis of these results, we assign the 3000 cm^{-1} peak observed at the α-$Al_2O_3(11\bar{2}0)/H_2O$ interface to the O−H stretch of (1) strongly hydrogen-bonded surface aluminol groups and/or (2) interfacial water molecules that are strongly hydrogen bonded to the alumina surface. IR pump−vSFG probe measurements of the interfacial OH species at the α-$Al_2O_3(11\bar{2}0)/H_2O$ interface reveal fast (bulk waterlike) vibrational relaxation dynamics, which is insensitive to changes in surface charge and ionic strength. This observation is in contrast to that reported for interfacial water at other charged surfaces like silica, where the vibrational relaxation dynamics are dependent on the surface charge and solution ionic strength. From these results, it is evident that the interfacial water at the α-$Al_2O_3(11\bar{2}0)$ surface is ordered and strongly hydrogen bonded. The presence 3000 cm^{-1} OH species could be the primary reason for the observation of very fast vibrational relaxation of strongly hydrogen bonded interface OH groups.

■ ASSOCIATED CONTENT

Supporting Information

The Supporting Information is available free of charge on the ACS Publications website at DOI: 10.1021/acs.jpcc.5b12486.

Hydrated α-$Al_2O_3(11\bar{2}0)$ configuration, vSFG setup, principle of vSFG spectroscopy, Fresnel factor correction of vSFG spectra, difference between PPP and SSP vSFG spectra, fitting of time-resolved vSFG data, and correlation between percent bleach and population transfer. (PDF)

■ AUTHOR INFORMATION

Corresponding Author

*E-mail: eborguet@temple.edu. Tel.: 1-215-204-9696. Fax: 1-215-204-9530.

Notes

The authors declare no competing financial interest.

■ ACKNOWLEDGMENTS

The authors acknowledge the National Science Foundation for supporting this work (NSF Grant CHE 1337880). The authors thank Professor M. Zdilla for alumina prism face orientation identification by X-ray diffraction and Mr. Steve Szewczyk at the University of Pennsylvania, Department of Materials Science and Engineering for gold coating of the alumina prism.

■ REFERENCES

(1) Jeffrey, G. A. *An Introduction to Hydrogen Bonding*; Oxford University Press: New York, 1997; Vol. *12*.

(2) Bakker, H.; Skinner, J. Vibrational Spectroscopy as a Probe of Structure and Dynamics in Liquid Water. *Chem. Rev.* **2010**, *110*, 1498−1517.

(3) Piatkowski, L.; Eisenthal, K.; Bakker, H. Ultrafast Intermolecular Energy Transfer in Heavy Water. *Phys. Chem. Chem. Phys.* **2009**, *11*, 9033−9038.

(4) Ramasesha, K.; Roberts, S. T.; Nicodemus, R. A.; Mandal, A.; Tokmakoff, A. Ultrafast 2D IR Anisotropy of Water Reveals Reorientation During Hydrogen-Bond Switching. *J. Chem. Phys.* **2011**, *135*, 054509.

(5) Asbury, J. B.; Steinel, T.; Kwak, K.; Corcelli, S.; Lawrence, C.; Skinner, J.; Fayer, M. Dynamics of Water Probed with Vibrational Echo Correlation Spectroscopy. *J. Chem. Phys.* **2004**, *121*, 12431−12446.

(6) Nibbering, E. T.; Elsaesser, T. Ultrafast Vibrational Dynamics of Hydrogen Bonds in the Condensed Phase. *Chem. Rev.* **2004**, *104*, 1887−1914.

(7) Isaienko, O.; Borguet, E. Ultra-Broadband Sum-Frequency Vibrational Spectrometer of Aqueous Interfaces Based on a Non-Collinear Optical Parametric Amplifier. *Opt. Express* **2012**, *20*, 547−561.

(8) Smits, M.; Ghosh, A.; Bredenbeck, J.; Yamamoto, S.; Müller, M.; Bonn, M. Ultrafast Energy Flow in Model Biological Membranes. *New J. Phys.* **2007**, *9*, 390.

(9) Hass, K. C.; Schneider, W. F.; Curioni, A.; Andreoni, W. The Chemistry of Water on Alumina Surfaces: Reaction Dynamics from First Principles. *Science* **1998**, *282*, 265−268.

(10) Furlong, B. K.; Hightower, J. W.; Chan, T. Y.-L.; Sarkany, A.; Guczi, L. 1, 3-Butadiene Selective Hydrogenation over Pd/Alumina and CuPd/Alumina Catalysts. *Appl. Catal., A* **1994**, *117*, 41−51.

(11) Flörsheimer, M.; Kruse, K.; Polly, R.; Abdelmonem, A.; Schimmelpfennig, B.; Klenze, R.; Fanghänel, T. Hydration of Mineral Surfaces Probed at the Molecular Level. *Langmuir* **2008**, *24*, 13434−13439.

(12) Boulesbaa, A.; Borguet, E. Vibrational Dynamics of Interfacial Water by Free Induction Decay Sum Frequency Generation (FID-SFG) at the $Al_2O_3(1120)/H_2O$ Interface. *J. Phys. Chem. Lett.* **2014**, *5*, 528−33.

(13) Ostroverkhov, V.; Waychunas, G. A.; Shen, Y. Vibrational Spectra of Water at Water/α-Quartz(0001) Interface. *Chem. Phys. Lett.* **2004**, *386*, 144−148.

(14) Becraft, K.; Richmond, G. In situ Vibrational Spectroscopic Studies of the CaF_2/H_2O Interface. *Langmuir* **2001**, *17*, 7721−7724.

(15) Dewan, S.; Yeganeh, M. S.; Borguet, E. Experimental Correlation Between Interfacial Water Structure and Mineral Reactivity. *J. Phys. Chem. Lett.* **2013**, *4*, 1977−1982.

(16) Jena, K. C.; Covert, P. A.; Hore, D. K. The Effect of Salt on the Water Structure at a Charged Solid Surface: Differentiating Second- and Third-order Nonlinear Contributions. *J. Phys. Chem. Lett.* **2011**, *2*, 1056−1061.

(17) Yang, Z.; Li, Q.; Chou, K. C. Structures of Water Molecules at the Interfaces of Aqueous Salt Solutions and Silica: Cation Effects. *J. Phys. Chem. C* **2009**, *113*, 8201−8205.

(18) Sung, J.; Shen, Y.; Waychunas, G. The Interfacial Structure of Water/Protonated α-$Al_2O_3(11\bar{2}0)$ as a Function of pH. *J. Phys.: Condens. Matter* **2012**, *24*, 124101.

(19) Sung, J.; Zhang, L.; Tian, C.; Shen, Y. R.; Waychunas, G. A. Effect of pH on the Water/α-$Al_2O_3(1102)$ Interface Structure Studied by Sum-Frequency Vibrational Spectroscopy. *J. Phys. Chem. C* **2011**, *115*, 13887−13893.

(20) Zhang, L.; Tian, C.; Waychunas, G. A.; Shen, Y. R. Structures and Charging of α-Alumina(0001)/Water Interfaces Studied by Sum-Frequency Vibrational Spectroscopy. *J. Am. Chem. Soc.* **2008**, *130*, 7686−7694.

(21) Catalano, J. G. Relaxations and Interfacial Water Ordering at the Corundum(110) Surface. *J. Phys. Chem. C* **2010**, *114*, 6624−6630.

(22) Catalano, J. G. Weak Interfacial Water Ordering on Isostructural Hematite and Corundum(001) Surfaces. *Geochim. Cosmochim. Acta* **2011**, *75*, 2062−2071.

DOI: 10.1021/acs.jpcc.5b12486
J. Phys. Chem. C XXXX, XXX, XXX−XXX

(23) Schlegel, M. L.; Nagy, K. L.; Fenter, P.; Sturchio, N. C. Structures of Quartz(100)- and (101)-Water Interfaces Determined by X-Ray Reflectivity and Atomic Force Microscopy of Natural Growth Surfaces. *Geochim. Cosmochim. Acta* **2002**, *66*, 3037−3054.
(24) Lee, W.; Lagerlof, K. Structural and Electron Diffraction Data for Sapphire (α-Al_2O_3). *J. Electron Microsc. Tech.* **1985**, *2*, 247−258.
(25) Le Caër, S.; Palmer, D. J.; Lima, M.; Renault, J. P.; Vigneron, G.; Righini, R.; Pommeret, S. Time-Resolved Studies of Water Dynamics and Proton Transfer at the Alumina-Air Interface. *J. Am. Chem. Soc.* **2007**, *129*, 11720−11729.
(26) Heilweil, E.; Casassa, M.; Cavanagh, R.; Stephenson, J. Vibrational Deactivation of Surface OH Chemisorbed on SiO_2: Solvent Effects. *J. Chem. Phys.* **1985**, *82*, 5216−5231.
(27) Woutersen, S.; Emmerichs, U.; Nienhuys, H.-K.; Bakker, H. J. Anomalous Temperature Dependence of Vibrational Lifetimes in Water and Ice. *Phys. Rev. Lett.* **1998**, *81*, 1106−1109.
(28) Yeganeh, M.; Dougal, S.; Pink, H. Vibrational Spectroscopy of Water at Liquid/Solid Interfaces: Crossing the Isoelectric Point of a Solid Surface. *Phys. Rev. Lett.* **1999**, *83*, 1179.
(29) Kresse, G.; Furthmueller, J. *VASP the Guide*; University of Vienna: Vienna, Austria, 2003.
(30) Kresse, G.; Furthmüller, J. Efficient Iterative Schemes for Ab Initio Total-Energy Calculations Using a Plane-Wave Basis Set. *Phys. Rev. B: Condens. Matter Mater. Phys.* **1996**, *54*, 11169.
(31) Blöchl, P. E. Projector Augmented-Wave Method. *Phys. Rev. B: Condens. Matter Mater. Phys.* **1994**, *50*, 17953.
(32) Kresse, G.; Joubert, D. From Ultrasoft Pseudopotentials to the Projector Augmented-Wave Method. *Phys. Rev. B: Condens. Matter Mater. Phys.* **1999**, *59*, 1758.
(33) Perdew, J. P.; Burke, K.; Ernzerhof, M. Generalized Gradient Approximation Made Simple. *Phys. Rev. Lett.* **1996**, *77*, 3865.
(34) Gan, W.; Wu, D.; Zhang, Z.; Feng, R. R.; Wang, H. F. Polarization and Experimental Configuration Analyses of Sum Frequency Generation Vibrational Spectra, Structure, and Orientational Motion of the Air/Water Interface. *J. Chem. Phys.* **2006**, *124*, 114705.
(35) Ostroverkhov, V.; Waychunas, G. A.; Shen, Y. R. New Information on Water Interfacial Structure Revealed by Phase-Sensitive Surface Spectroscopy. *Phys. Rev. Lett.* **2006**, *94*, 046102.
(36) Chandrasekharan, R.; Zhang, L.; Ostroverkhov, V.; Prakash, S.; Wu, Y.; Shen, Y.-R.; Shannon, M. A. High-Temperature Hydroxylation of Alumina Crystalline Surfaces. *Surf. Sci.* **2008**, *602*, 1466−1474.
(37) Huang, P.; Pham, T. A.; Galli, G.; Schwegler, E. Alumina-(0001)/Water Interface: Structural Properties and Infrared Spectra from First-Principles Molecular Dynamics Simulations. *J. Phys. Chem. C* **2014**, *118*, 8944−8951.
(38) Kubicki, J.; Apitz, S. Molecular Cluster Models of Aluminum Oxide and Aluminum Hydroxide Surfaces. *Am. Mineral.* **1998**, *83*, 1054−1066.
(39) Nanjundiah, K.; Hsu, P. Y.; Dhinojwala, A. Understanding Rubber Friction in the Presence of Water Using Sum-Frequency Generation Spectroscopy. *J. Chem. Phys.* **2009**, *130*, 024702.
(40) Ram, S. Infrared Spectral Study of Molecular Vibrations in Amorphous, Nanocrystalline and AlO(OH)·αH_2O Bulk Crystals. *Infrared Phys. Technol.* **2001**, *42*, 547−560.
(41) Zhuravlev, L. The Surface Chemistry of Amorphous Silica. Zhuravlev Model. *Colloids Surf., A* **2000**, *173*, 1−38.
(42) Baumgarten, E.; Wagner, R.; Lentes-Wagner, C. Quantitative Determination of Hydroxyl Groups on Alumina by IR Spectroscopy. *Fresenius' Z. Anal. Chem.* **1989**, *334*, 246−251.
(43) Kirsch, H.; Wirth, J.; Tong, Y. J.; Wolf, M.; Saalfrank, P.; Campen, R. K. Experimental Characterization of Unimolecular Water Dissociative Adsorption on alpha-Alumina. *J. Phys. Chem. C* **2014**, *118*, 13623−13630.
(44) Lindner, J.; Vöhringer, P.; Pshenichnikov, M. S.; Cringus, D.; Wiersma, D. A.; Mostovoy, M. Vibrational Relaxation of Pure Liquid Water. *Chem. Phys. Lett.* **2006**, *421*, 329−333.
(45) Lock, A.; Bakker, H. Temperature Dependence of Vibrational Relaxation in Liquid H_2O. *J. Chem. Phys.* **2002**, *117*, 1708−1713.
(46) Lock, A. J.; Woutersen, S.; Bakker, H. J. Ultrafast Energy Equilibration in Hydrogen-Bonded Liquids. *J. Phys. Chem. A* **2001**, *105*, 1238−1243.
(47) Eftekhari-Bafrooei, A.; Borguet, E. Effect of Surface Charge on the Vibrational Dynamics of Interfacial Water. *J. Am. Chem. Soc.* **2009**, *131*, 12034−12035.
(48) McGuire, J. A.; Shen, Y. R. Ultrafast Vibrational Dynamics at Water Interfaces. *Science* **2006**, *313*, 1945−1948.
(49) Eftekhari-Bafrooei, A.; Borguet, E. Effect of Electric Fields on the Ultrafast Vibrational Relaxation of Water at a Charged Solid−Liquid Interface as Probed by Vibrational Sum Frequency Generation. *J. Phys. Chem. Lett.* **2011**, *2*, 1353−1358.
(50) Woutersen, S.; Bakker, H. J. Resonant Intermolecular Transfer of Vibrational Energy in Liquid Water. *Nature* **1999**, *402*, 507−509.
(51) Deàk, J. C.; Rhea, S. T.; Iwaki, L. K.; Dlott, D. D. Vibrational Energy Relaxation and Spectral Diffusion in Water and Deuterated Water. *J. Phys. Chem. A* **2000**, *104*, 4866−4875.
(52) Kropman, M. F.; Nienhuys, H.-K.; Woutersen, S.; Bakker, H. J. Vibrational Relaxation and Hydrogen-Bond Dynamics of HDO:H_2O. *J. Phys. Chem. A* **2001**, *105*, 4622−4626.
(53) Eftekhari-Bafrooei, A.; Borguet, E. Effect of Hydrogen-Bond Strength on the Vibrational Relaxation of Interfacial Water. *J. Am. Chem. Soc.* **2010**, *132*, 3756−3761.
(54) Deàk, J. C.; Pang, Y.; Sechler, T. D.; Wang, Z.; Dlott, D. D. Vibrational Energy Transfer Across a Reverse Micelle Surfactant Layer. *Science* **2004**, *306*, 473−476.
(55) Flores, S. C.; Kherb, J.; Konelick, N.; Chen, X.; Cremer, P. S. The Effects of Hofmeister Cations at Negatively Charged Hydrophilic Surfaces. *J. Phys. Chem. C* **2012**, *116*, 5730−5734.
(56) Kropman, M. F.; Bakker, H. J. Effect of Ions on the Vibrational Relaxation of Liquid Water. *J. Am. Chem. Soc.* **2004**, *126*, 9135−9141.
(57) Dove, P. M. The Dissolution Kinetics of Quartz in Sodium Chloride Solutions at 25 Degrees to 300 Degrees C. *Am. J. Sci.* **1994**, *294*, 665−712.

DOI: 10.1021/acs.jpcc.5b12486
J. Phys. Chem. C XXXX, XXX, XXX−XXX